*AAPS PharmSciTech, Vol. 15, No. 3, June 2014 (© 2014)*
DOI: 10.1208/s12249-014-0092-0

*Review Article*

*Theme: Advances in Formulation and Device Technologies for Pulmonary Drug Delivery*
*Guest Editors: Paul B. Myrdal and Steve W. Stein*

# Mechanisms of Pharmaceutical Aerosol Deposition in the Respiratory Tract

**Yung Sung Cheng**[1,2]

*Received 7 August 2013; accepted 21 January 2014; published online 22 February 2014*

***Abstract.*** Aerosol delivery is noninvasive and is effective in much lower doses than required for oral administration. Currently, there are several types of therapeutic aerosol delivery systems, including the pressurized metered-dose inhaler, the dry powder inhaler, the medical nebulizer, the solution mist inhaler, and the nasal sprays. Both oral and nasal inhalation routes are used for the delivery of therapeutic aerosols. Following inhalation therapy, only a fraction of the dose reaches the expected target area. Knowledge of the amount of drug actually deposited is essential in designing the delivery system or devices to optimize the delivery efficiency to the targeted region of the respiratory tract. Aerosol deposition mechanisms in the human respiratory tract have been well studied. Prediction of pharmaceutical aerosol deposition using established lung deposition models has limited success primarily because they underestimated oropharyngeal deposition. Recent studies of oropharyngeal deposition of several drug delivery systems identify other factors associated with the delivery system that dominates the transport and deposition of the oropharyngeal region. Computational fluid dynamic simulation of the aerosol transport and deposition in the respiratory tract has provided important insight into these processes. Investigation of nasal spray deposition mechanisms is also discussed.

**KEY WORDS:** aerosol deposition; drug delivery; inhalation; lung.

## INTRODUCTION

Delivery of a therapeutic agent by inhalation has seen increasing applications for many respiratory diseases, including asthma, COPD, allergies, and influenza. Aerosol delivery has advantages: it delivers medication directly to where it is needed and it avoids the first-pass effect with minimum reduction of bioavailability. In addition, the inhalation route has been extensively researched as an alternative for systematic administration of proteins and peptides because of the large surface area in the pulmonary region and rapid absorption of the delivered drug from the alveolar region to the blood. Aerosol delivery is noninvasive and is effective in much lower doses than required for oral administration. Currently, there are several types of therapeutic aerosol delivery systems, including the pressurized metered-dose inhaler (pMDI), the dry powder inhaler (DPI), the medical nebulizer, the solution mist inhaler, and nasal sprays.

Following inhalation therapy, only a fraction of the dose reaches the expected target area. Knowledge of the amount of drug actually deposited is essential in designing the delivery system or devices to optimize the delivery efficiency to the targeted region of the respiratory tract. This knowledge is essential in developing a dosing regimen to deliver the required amount of active compound to the patient. It is also important in determining the range of doses necessary for preclinical toxicology studies and for comparing the efficiency of delivery among different delivery devices. Newman showed through case studies that the clinical effects of an asthma treatment can be correlated directly with the deposited dose in the lung (1). Derom and Pauwels also reached similar conclusions (2). Lung deposition data are very useful to show the bioequivalence between two pMDIs and DPIs or between a new device and an existing device. Deposition data obtained using human volunteers or physical models of airways are often included in the development of inhalation drugs (3). Standardized techniques of obtaining human deposition data using planar image and single-photon emission tomography for orally inhaled pharmaceutical products are available (4,5).

The transport and deposition of aerosol in the human respiratory tract have been studied over the past 50 years, primarily for assessing inhalation dosimetry of ambient and occupational aerosols (6,7). Based on these studies, the aerosol transport and deposition mechanisms are well understood. The deposition pattern can be influenced by several factors: (1) particle characteristics, such as particle size, shape, density, charge, and hygroscopicity; (2) airway geometry as a function of gender, age, and diseases status; and (3) breathing pattern, including frequency, tidal volume, and breath-holding time. The primary aerosol deposition mechanisms may include

[1] Lovelace Respiratory Research Institute (LRRI), 2425 Ridgecrest, SE, Albuquerque, New Mexico 87108, USA.
[2] To whom correspondence should be addressed. (e-mail: ycheng@lrri.org;)

inertial impaction, sedimentation, diffusion, interception, and electrostatic effects (6,8,9). The contribution of these deposition mechanisms is a function of particle size and flow rate in a given region of respiratory tract.

Lung deposition models have been used extensively to estimate radiation doses from occupational and ambient exposure to radioactive aerosols as well as inhalation doses of hazardous particulate matter in different environments. There were also attempts to use these models or others to investigate factors that may affect aerosol drug delivery (3,10–12). However, prediction of regional deposition of pharmaceutical aerosol using these models has limited success primarily because they underestimate oropharyngeal deposition (3,11), which also leads the overestimation of lung deposition. Current studies of oropharyngeal deposition of several drug delivery systems identify other factors including mouthpiece diameter, particle velocity, and electrostatic effects associated with the delivery system that dominates the transport and deposition of the oropharyngeal region (9,13–16). Computational fluid dynamic (CFD) simulation of the aerosol transport and deposition in the respiratory tract has provided important insight into these processes.

## DEPOSITION IN THE RESPIRATORY TRACT

The human respiratory tract is a complex system. Aerosol deposition in the lung has been studied *in vivo* using human volunteers (17–19); *in vitro* using physical airway replicas (20–22); and theoretically using mathematical models (23). In these studies, the respiratory tract is usually divided into three major regions including the extrathoracic, thoracic, and pulmonary regions. The human respiratory tract can be divided into three anatomical regions as shown in Fig. 1. The extrathoracic or head airway including the naso-oro-pharyngo-laryngeal region is the entry to the respiratory tract and the first defense against hazardous inhaled material. The tracheobronchial (TB) tree or conducting airway includes the trachea and 16 generations of branching airways. Gas exchange takes place in the pulmonary region (P), which consists of alveolar ducts and alveolar sacs. Most people breathe through the nose when at rest or during light exercise, but switch to oral/nasal breathing during heavy exercise or work. People make this switch to oral/nasal breathing because resistance through the oral airway is much lower than through the nasal airways. Some people are habitual oral breathers even at rest.

When an airborne particle is transported near a person, it may be inhaled and enters the respiratory tract through either nasal or oral passages. The ability of the particle to enter the head airway, also known as its inhalability, is a function of its aerodynamic diameter. Inhalability is a fraction of airborne particles entering the human airway. Most of the experimental data on inhalability has been obtained in aerosol wind tunnels. Inhalability has been found to be near 100% for particles smaller than 5 μm, based on these wind tunnel studies (24). The inhalability decreases as the particle size increases and stays at 50% for particles greater than about 50 μm (24,25).

Once the particle enters the respiratory tract *via* either the nose or mouth, it may be deposited in different regions of the respiratory tract. During breathing, the air flow undergoes several direction changes in the nasal/mouth, pharynx, larynx regions, and airway bifurcations. Larger particles (>0.5 μm)

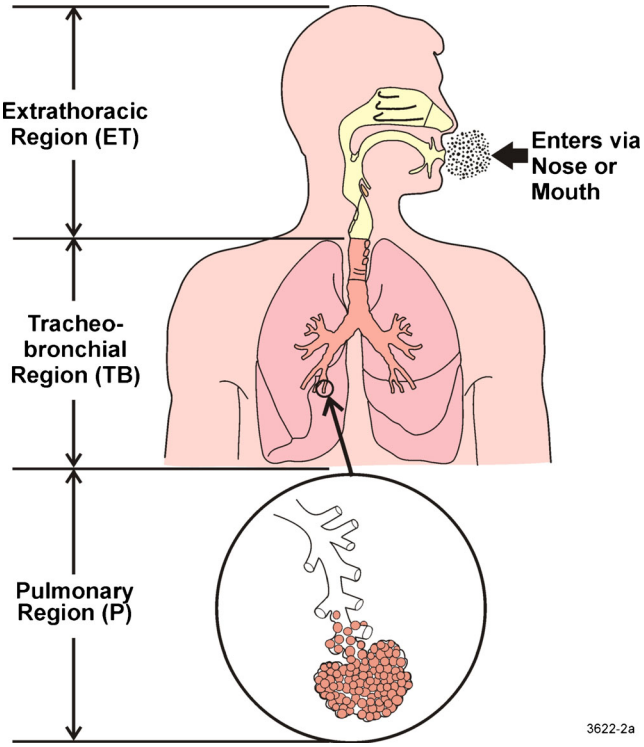


**Fig. 1.** A schematic diagram of the human respiratory tract

may deposit by impaction in these regions because they could not follow the air streamline. In fact, deposition by impaction in the oropharyngeal region remains a major portion of the emitted dose for pMDI and DPI devices. In the small airways and alveolar region, deposition by sedimentation is the major deposition mechanism of inhaled particles. On the other hand, small particles (<0.2 μm) may be deposited by diffusion in all regions of the respiratory tract. Diffusion deposition is important for nanoparticles <100 nm. Interception deposition is important for elongated particles such as fibrous aerosols when the long particle dimension is comparable with the pulmonary airway dimension. Pharmaceutical aerosol may carry electrostatic charges during the generation and transport of the aerosol, especially for DPI and pMDI devices (26). Although the aerosol charge status may vary with many factors including the material, expedients, formulation, and material used in the devices, the amount of electrostatic charges on aerosol from several devices was deemed to affect the deposition. Electrostatic effects including image and space charge forces are found to enhance particle deposition if the number of charges on particles exceeds a threshold (9,27–30). Condensation of water in the humid environment of the respiratory tract may cause particles to grow and change the way that they move through the respiratory tract.

The efficiency of particle deposition and the spatial distribution of deposition in the human respiratory tract have been measured experimentally in human volunteers and physical models of airway replicas using spherical test particles tagged with radiolabels or fluorescent materials. Lung deposition models, such as those developed by the International Commission for Radiation Protection (ICRP) and the National Council on Radiation Protection and Measurements (NCRP), are based on airway anatomy and breathing patterns

of standard men (6,7). These models have been used extensively to estimate the radiation dose as a result of exposure to radioactive aerosols as well as inhalation dosimetry of hazardous particulate matter in the ambient and occupational environments. Theoretical models utilize simplified airway geometries and aerosol deposition mechanisms including impaction, sedimentation, diffusion, and interception to derive deposition equations in each of the airway regions. Total and regional aerosol depositions are then calculated with input information of particles with known characteristics (size, density, and shape) and physiological conditions (tidal volume and breathing rate). Experimental data obtained *in vivo* and *in vitro* were used to verify the deposition equations or regional and total deposition in the respiratory tract. ICRP and NCRP as well as other lung deposition models have been extensively verified by the available data (6,7).

The deposition fractions are a function of aerodynamic diameter in men with nasal breathing for a tidal volume of 1.25 L and 20 breaths/min (Fig. 2). The plot shows that, for particles larger than 0.2 μm in diameter, deposition in the nasal and laryngeal region increases as particle size increases up to 8 μm due to the inertial mechanism. On the other hand, nasal and laryngeal deposition also increases when particle size decreases from 0. 2 μm because of the mechanism of diffusion. Nasal deposition decreased slightly for particles greater than 8 μm because of decreasing inhalability of large particles. Particles greater than 10 μm in diameter are deposited primarily in the nasal airways with little penetration to the lung. Particles in the size range between 0.002 and 6 μm can penetrate into lower airways and deposit in the pulmonary regions. Deposition fractions are a function of aerodynamic diameter in man with mouth breathing for a tidal volume of 1.25 L and 20 breaths/min (Fig. 3). One major difference in mouth breathing as opposed to nasal breathing is that deposition in the oral airway is much less than the deposition in the nasal airway for particles of all sizes between 0.01 and 10 μm. As a result, there is substantial deposition in the TB and P regions when mouth breathing is the primary inhalation method. Therefore, pharmaceutical devices for pulmonary delivery such as pMDIs, DPIs, and nebulizers are generally delivered *via* oral inhalation to reduce deposition in the head airway and

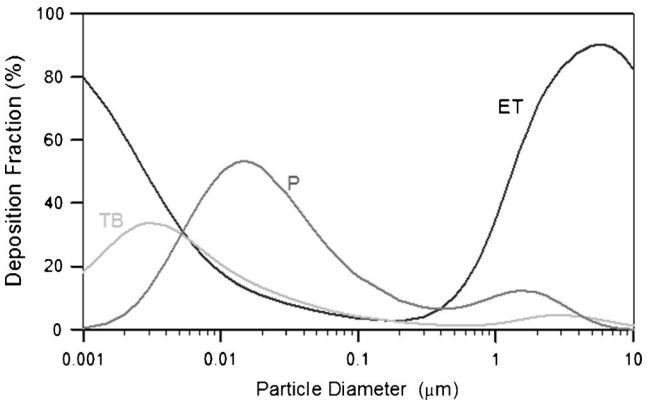


**Fig. 2.** Distribution of particle deposition for different regions of the respiratory tract system for 100% nasal breathing. The data were calculated using the LUDEP software (NRPB, Oxon, UK) based on the ICRP model (6)

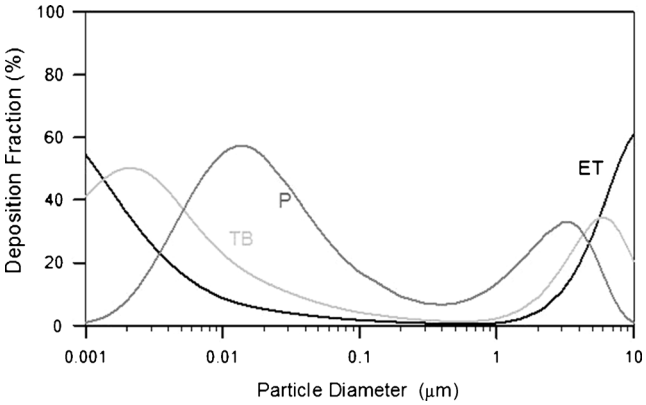


**Fig. 3.** Distribution of particle deposition for different regions of the respiratory tract system for 100% mouth breathing. The data were calculated using the LUDEP software (NRPB, Oxon, UK) based on the ICRP model (6)

maximize dose to the lower airways. On the other hand, nasal sprays are designed to deposit in the nasal passages for local treatments. Human deposition data has been used as the technical basis to formulate the size selection criteria of sampling methods for designing particulate samplers such as PM10, inhalable, and respirable samplers (24). The information is also used for the design of aerosol drug delivery systems.

## INHALATION DRUG DELIVERY

The inhalation delivery route of pharmaceutical drugs including nasal and oral delivery depends on the target regions of the drugs. Nasal sprays and other devices are used to deliver drugs into the nasal cavity using the nasal inhalation route for local decongestion, influenza vaccines, or to ameliorate allergic conditions. Other aerosol drugs targeting tracheobronchial and pulmonary airways to treat respiratory diseases such as asthma, cystic fibrosis, COPD, tuberculosis, and allergies are delivered by the oral inhalation route because particle deposition or losses in the extrathoracic region are much lower for oral inhalation compared to nasal inhalation as shown in Fig. 3. More recently, inhalation delivery has been extensively researched as an alternative for systematic administration of proteins and peptides. This inhalation delivery has been done primarily by oral inhalation for delivery to the pulmonary region. In addition, this inhalation delivery has also been carried out by nasal inhalation to the nasal cavity to be absorbed and transferred to the circulation.

Estimates of lung deposition patterns from the deposition models have been used as a general guide in the design of aerosol drug delivery. For example, for pulmonary delivery, the optimal particle size is frequently assigned between 3 and 5 μm based on the deposition curve for mouth breathing (Fig. 3). This emphasis of particle size leads to an *in vitro* test of particle size of fine particle fraction (FPF), which is defined roughly as the mass fraction of particles with an aerodynamic diameter <5 μm (31,32). The FPF is usually estimated by measuring particle size *in vitro* using inertial instruments (33). The most common inertial instruments used in the pharmaceutical industry are the Andersen cascade impactors (ACI) (Model Mark II, Andersen Instruments, Thermo

Andersen, Smyrna, GA) and the Next Generation Cascade Impactors (MSP Co., Minneapolis, MN). In Europe, a multistage liquid impinger (MLI, Copley Scientific Limited, Nottingham, UK) is also used. Depending on the instrument, the FPF is calculated differently. The FPF calculated from the ACI operating at 28.3 L $min^{-1}$ is the portion of the particles <4.7 μm (fraction of mass collected from stages 3–7 and the back-up filter), whereas for the MLI operating at 60 L $min^{-1}$, it is <6.8 μm (fraction of mass collected at stages 3 and 4). Therefore, the FPF calculated from the MLI is greater than that of the ACI.

The FPF has been used to correlate the *in vivo* deposition obtained by gamma scintigraphy. The gamma scintigraphy techniques use a radiolabeled drug and provide quantitative information on the fraction of aerosol delivered to different regions of lung, including the nasal cavity, orophyarnx, lung, and expired air, as well as deposition in the device and/or spacer (32). The deposition pattern in the lung can be further divided into two or three regions of interest, generally including a central and a peripheral region and often including a third "intermediate region" (34). Clark showed that changes in FPF produced by different spacer devices are mirrored by changes in lung deposition (35). In a more extensive study of pMDIs, DPIs, and soft mist inhalers, Newman compared various measurements of FPFs from ACIs and MLIs with *in vivo* lung deposition data (32). There is a correlation between the lung deposition fraction and the FPF defined as <5 μm (Fig. 4); however, the FPF always overestimates the true lung deposition fraction obtained by *in vivo* technique. The mass fraction of stage 4 (<3.3 μm) on the MLI has a much better predictive value for *in vivo* deposition in the lung. The impinger data in Newman's analysis generally failed to correctly predict the relationship between the lung deposition from an MDI compared with another devices. He concluded that FPF data alone are unreliable as a predictor of the relative deposition from two devices with markedly different spray characteristics (*e.g.*, pMDI *versus* DPI).

## DOSE ESTIMATE USING THE LUNG DEPOSITION MODEL

Attempts have been made to estimate lung deposition efficiency directly from *in vitro* measurement of particle size distribution and breathing rates. Clark *et al.* compared oropharyngeal deposition data of several pMDI and DPI studies obtained with gamma scintigraphy with the empirical oral deposition model of a published model (13). The actual oral deposition and model prediction were correlated but were in disagreement in terms of absolute magnitude, with actual oropharyngeal deposition being approximately 60% to 70% more than predicted.

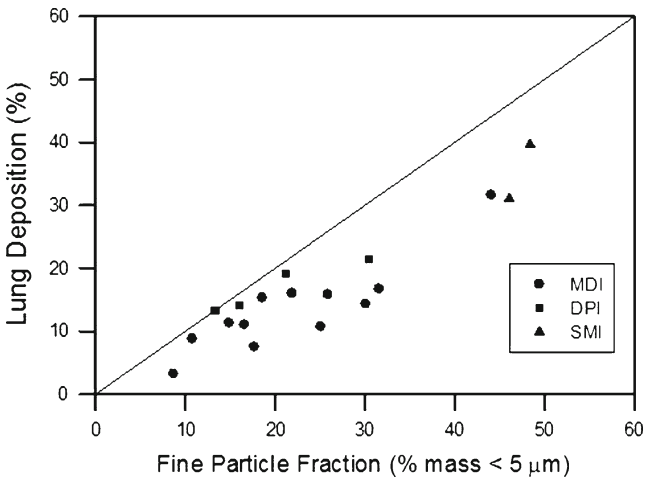


**Fig. 4.** Correlation of lung deposition with the fine particle fraction (32). *MDI* = metered-dose inhaler; *DPI* = dry powder inhaler; *SMI* = soft mist inhaler

Because aerosol drug delivery is different from the natural breathing of particulate matter, modifications of existing lung deposition model are needed. This includes 100% inhalability because the nasal or oral delivery device is placed inside the nasal or oral cavity. Also, deposition in delivery devices ranging from a few percent for DPI to over 60% for nebulizers needs to be accounted for. The third modification is the estimated oropharyngeal deposition for oral delivery. Following the suggestion made by Pritchard *et al.*, the fraction of particles collected in the impactor/impinger inlet (*i.e.*, United States Pharmacopoeia (USP) or glass throats) was assigned as a part of the deposition fraction in the oropharyngeal region (11). The individual fraction of particles in the impactor/impinger stage was used to calculate the deposition fraction in the regional deposition. The sum of the calculated deposition in the oropharyngeal region from the individual size increments of the impactor/impinger was added to the measured deposition fraction from the USP induction port or glass inlet to the impactor/impinger. The total was then the calculated deposition fraction in the oropharyngeal region. Based on these modifications, the Lung Dose Evaluation Program (LUDEP) software was used to estimate the deposition pattern of pulmonary delivery of pharmaceutical aerosol *via* mouth breathing and compared *in vivo* deposition pattern obtained with gamma scintigraphy (3,6,12).

Data from a gamma scintigraphic study of three Pari nebulizers (36) were used for comparison of values calculated by LUDEP. The droplet size distribution was measured using the Malvern 2600 laser diffraction technique (Malvern Instruments). The mass median diameters (MMDs) were between 4 and 5.5 μm. The GSD of 2.1 was assumed based on another report (37). Ten healthy adult volunteers took part in the study. They were instructed to inhale from the nebulizer with relax tidal volumes for 15 min. Breathing information was not reported. A breathing rate or minute volume of 15 L and a frequency of 16 $min^{-1}$ were assumed. The nebulizers were filled with 3 mL of $^{99m}$Tc-labeled diethylenetriaminepentaacetic acid solution. Table I shows the comparison of the deposition pattern for the Pari LC nebulizer operated in the intermittent mode. The MMD was 4.0 μm for the Pari LC nebulizer. The deposition pattern showed that 61.5% of the radioactivity remained in the nebulizer. The oropharyngeal deposition was 10.9%, and the lung deposition was 15.3%. The deposition calculated by the LUDEP software showed 8.2% and 16.7% deposited in the oropharyngeal region and lung with 13.5% in the expired air. The regional deposition patterns and fraction of expired air of the calculated values were within the range of the experimental error, indicating good agreement. Similar results were obtained for several other nebulizers having similar particle sizes, indicating good agreement between the predicted deposition patterns and agreed with *in vivo* data (3,12). In these studies, the oropharyngeal deposition was relatively small, <15% of the emitted dose.

Several *in vivo* deposition studies of pMDIs using either chlorofluorocarbon (CFC) or hydrofluorocarbon (HFA) propellants are summarized in Cheng (3). Table I shows the comparison of *in vivo* deposition pattern and the deposition calculation of beclomethasone dipropionate (BDP) using CFC and HFA formulations reported in healthy volunteers (38). The CFC-BDP had 10%, 81%, 6.3%, and 2.7% deposition in the actuator, oropharynx, lung, and expired air, respectively, whereas for the HFA-BDP, the deposition was 15%, 25%, 47%, and 13%, in the actuator, oropharynx, lung, and expired air, respectively. For the HFA-BDP, deposition in the oropharynx was much lower than the CFC-BDP, resulting in higher lung deposition and expired air. The calculated deposition patterns shown in Table I for lung and oropharyngeal deposition were outside the error bars of the *in vivo* data, indicating that they were not in good agreement. Additional *in vivo* data were also used for comparison, for deposition in the lung and oropharyngeal region (39–43). In general, the LUDEP method underestimated the oropharyngeal deposition and overestimated the lung deposition and drug expiration. The high oropharyngeal deposition (20–80%) for pMDI delivery obtained *in vivo* was verified for *in vitro* studies using realistic human oral airway replica (44,45).

DPIs including Spinhaler, Rotahaler, Diskhaler, and Turbuhaler use inspiratory flow to aerosolize the powder and the rotor, screen, or flow path to create turbulence in order to break up aggregates and reduce the particle size. A high peak inspiratory flow rate (>60 L $min^{-1}$) is recommended to increase air turbulence for enhancing powder deagglomeration. An example is the deposition pattern of the budesonide inhaled *via* the Turbulhaler in healthy subjects (46). Table I shows a deposition pattern of 67%, 15%, and 0.5% at the oropharynx, lung, and expired air for a slow inhalation maneuver at 36 L $min^{-1}$. The predicted deposition shows lower oropharyngeal and higher lung deposition than the experimental data. Additional *in vivo* deposition data using DPIs were also used for comparison (3,12,39,47–49). In general, the LUDEP method underestimated the oropharyngeal deposition.

In summary, the application of existing lung models developed for inhalation of particulate matter in the ambient or occupational environments for dose estimates of pharmaceutical aerosols for pulmonary delivery *via* mouth breathing has mixed results. While the model adequately predicted deposition dose in aerosol delivery using nebulizers, prediction for aerosol delivery using both DPIs and pMDIs was not satisfactory. Deposition of pharmaceutical aerosol by DPIs and pMDIs in the oropharyngeal region was high and in some cases over 60%. In contrast, lower deposition (<20%) was seen in the same region for inhaling ambient or occupational particulate matter. The high deposition in the oropharyngeal region reduces the amount of drugs getting to the targeted tissue in the lower airway. This may cause side effects and defeat the purpose of oral route of inhalation for pulmonary delivery.

## DEPOSITION IN THE OROPHARYNGEAL REGIONS

Recent understandings of the aerosol transport and deposition processes in the oropharyngeal regions have made substantial progress through studies in realistic upper airway replicas and CFD simulation. Studies with airway replicas made from cadaver or MRI scans provided reproducible deposition data which can be used to study the deposition mechanism. Realistic airway geometry has also been used in the CFD simulation to study the air flow and deposition processes.

An adult oral airway replica including an oral cavity and laryngeal and tracheal airway was casted from an alginate dental impression of a living Caucasian male adult; it represented approximately 50% of the full opening (50). Detailed airway dimensions in 0.3-cm intervals were reported. This Lovelace Respiratory Research Institute (LRRI) replica was used in the *in vitro* studies of nanoparticle deposition and coarse particle deposition of micro-metered sizes using standard test aerosols at constant inspiratory flow rates (20,50). The deposition efficiency for flow rates of 15, 30, and 60 L $min^{-1}$ was plotted as a function of the impaction parameter (Fig. 5). The deposition data showed a monotonic increase with the impaction parameter, indicating that impaction is the dominant deposition mechanism in the oropharyngeal airway. The deposition efficiency is also in the same range of data obtained in the *in vivo* deposition results as shown in Fig. 6. This oral airway geometry has been used in the CFD simulation to study the flow and aerosol transport (51–54). Figure 7 shows the flow pattern in the oropharyngeal airway model at an inspiratory flow rate of 15 L $min^{-1}$ (51). The primary characteristics of the axial flow fields are skewed velocity profiles with the maximum velocity shifted to the outer bend generated by the centrifugal force in the curved

**Table I.** Deposition Patterns of Nebulizer (36), pMDIs (38), and Turbuhaler (46) and Calculation

| | | Device/actuactor/ mouthpiece (%) | Oropharyngeal region (%) | Lung (%) | Expired air (%) |
|---|---|---|---|---|---|
| Nebulizer | Measurement | 61.5±16 | 10.9±6.5 | 15.3±12.8 | 12.2±2.4 |
| | Calculation | 61.5 | 8.2 | 16.7 | 13.5 |
| pMDI-CFC | Measurement | 10 | 81.0±12.6 | 6.3±2.7 | 2.7±0.9 |
| | Calculation | 10 | 64.70 | 17.20 | 8.10 |
| pMDI-HFA | Measurement | 15 | 24.7±11.0 | 46.8±10.2 | 13.5 ±3.4 |
| | Calculation | 15 | 37.0 | 18.3 | 29.7 |
| DPI | Measurement | 18.1±6.4 | 66.7±8.0 | 14.8±3.3 | 0.5±0.4 |
| | Calculation | 18.1 | 49.5 | 27.0 | 5.4 |

*pMDI-CFC* pressurized metered-dose inhaler-chlorofluorocarbon, *pMDI-HFA* pressurized metered-dose inhaler-hydrofluorocarbon, *DPI* dry powder inhaler

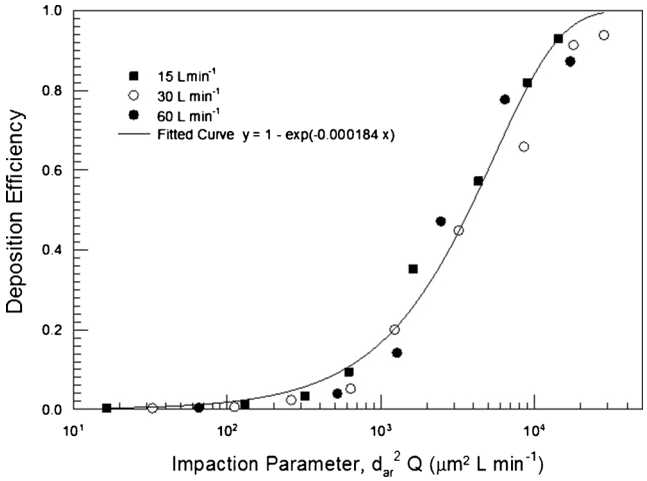


**Fig. 5.** Oral deposition efficiency in a human airway replica as a function of the impaction parameter and flow rate (20). The *solid curve* is the best-fitted curve

portion from the oral cavity to the pharynx. There are also secondary flows in the oral cavity. Deposition efficiency obtained from the CFD simulation agreed well with the experimental data. These studies show that inertial impaction by the curved streamline of the main flow in the oropharyngeal region at the rear of the oral cavity and deposition caused by a constriction in the larynx is the dominant deposition mechanism.

Stapleton *et al.* developed an idealized mouth–throat replica at the University of Alberta (55). This model is an average geometrical mouth–throat based on data from a CT scan, MRI scan, and living subjects. This idealized model has been the basis of many deposition studies, including deposition in aerosol drug delivery devices (14,56,57). A recent study showed that aerosol deposition in the idealized replica is in close agreement with those in the LRRI realistic mouth–throat replica for liquid aerosol and solid aerosol when the idealized replica is coated to prevent particle bounce (58). The same study also showed that the deposition in USP induction port was much lower.

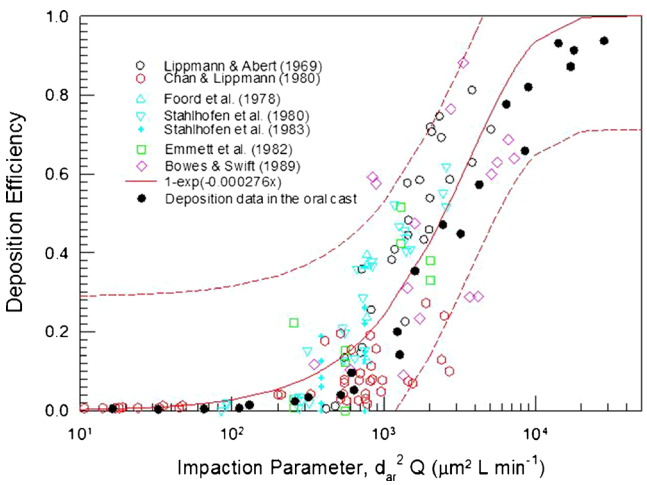


**Fig. 6.** Comparison of oral deposition in the replica with reported *in vivo* deposition data. The *solid curve* is the best-fitted curve for the *in vivo* data, and the *dashed curves* are fitted curves with ±SD (with permission from Cheng *et al.* 20)

## ORAL DEPOSITION FOR THE DPIS

Data obtained with gamma scintigraphy of several DPIs showed that the oropharyngeal depositions were 60% to 70% higher than predicted using the oral deposition model in the existing human lung deposition model (13). They suggested that one reason for the high oropharyngeal deposition may be caused by the mouthpiece design of DPIs. DeHaan and Finlay studied the deposition of monodisperse aerosol using two DPIs (Diskus and Turbuhaler), two nebulizers, a metered-dose inhaler with holding chamber, and a straight tube with 17-mm diameter for flow rate of 5 to 90 L $min^{-1}$ (14). Oropharyngeal deposition in an idealized mouth and throat model was measured. Oropharyngeal deposition for two nebulizers using a pMDI/holding chamber was not different from the deposition of the straight tube. However, deposition for the two DPIs was significantly higher than the straight tube, up to 14 times higher. The mouthpiece inner diameter of various DPIs ranged from 5 to 12 mm smaller than those used for *in vivo* and *in vitro* studies of oral deposition.

In a follow-up study, DeHaan and Finlay measured deposition in an idealized oral cavity replica (15). Aerosol was delivered through inlets with diameters ranging from 3, 5, 8, 11, 14, to 17 mm and flow rates of 15 to 90 L $min^{-1}$. The results were shown for a given particle size and flow rate: aerosol deposition increased with decreasing inlet diameter. Observation of deposition pattern indicated that deposition is centered on the rear upper surface of the oral cavity along the axis of the inlet nozzles for all inlets except the largest one (17 mm). CFD simulation of the flow pattern using the same oral cavity geometry and aerosol inlets of 3, 5, and 8 μm clearly showed an air jet from the inlet impinging on the back of the mouth (Fig. 8) (56). Deposition efficiency does not correlate with the impaction diameter, $d_{ae}^2Q$, which does not include the inlet diameter. The results correlate with the Stokes number based on the inlet diameter ($D_{inlet}$) and jet velocity at impact point (($U_{c,\ jet}$), $St = d_{ae}^2 C\ U_{c,\ jet}/18\mu D_{inlet}$) (15). They also performed deposition in the same oral replica for six commercial DPIs, and the deposition results follow the same empirical equation. These studies prove that deposition by the impinging turbulent jet from the narrow diameter of the DPI mouthpiece is the main mechanism for the enhanced deposition in the oropharyngeal region.

## ORAL DEPOSITION FOR THE PMDI

*In vivo* deposition and deposition in replicas show that 80% to 90% of pharmaceutical aerosol was deposited in the oropharyngeal region for pMDIs with the CFC propellant (Table I). The oropharyngeal deposition for pMDIs with the HFA formulation decreases substantially to between 50% and 70%. In addition, the oropharyngeal deposition does not increase with the inspiratory flow rate, indicating that the

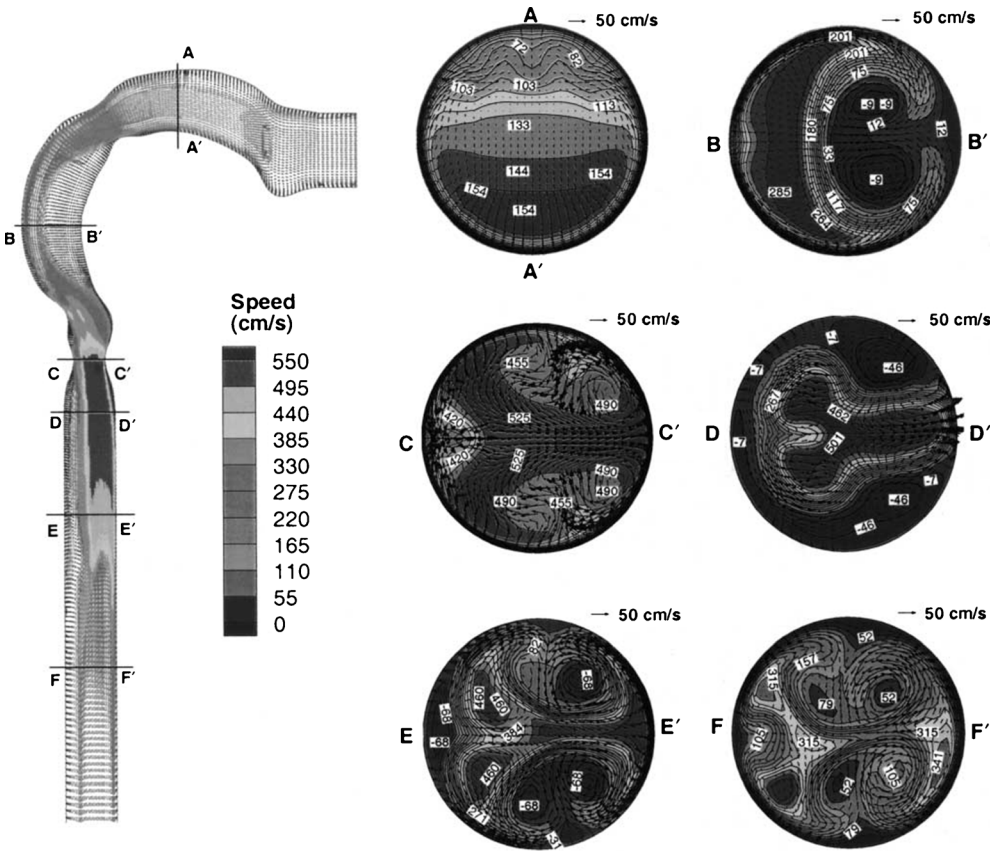


**Fig. 7.** Velocity profiles in the oral airway model at $Q$=15 L min$^{-1}$. The *left panel* exhibits midplane ($y$=0 plane) velocity contours with uniform velocity vectors. The *right panel* shows the axial velocity contours (magnitudes in centimeters per second) and secondary velocity vectors at different cross sections (with permission from Kleinstreuer and Zhang (51)

impaction model based on the bulk inspiratory flow in the oral cavity cannot explain the deposition mechanism. In a pMDI device, when the canister valve is actuated, a metered volume of highly pressurized fluid containing the drug and propellant is released through a small nozzle (typically 0.5 mm for the CFC formulations and 0.25 mm for the HFA formulations). The nozzle exit velocity is very high, between 150 and 225 m s$^{-1}$ (16). In a report, the spray velocity of the aerosol plume at 10 cm from the nozzle exit was measured for several commercial pMDIs (59). The mean spray velocity for four CFC formulations and two HFA formulations was between 5.1 and 8.4 m s$^{-1}$, and for the other three HFA formulations, the mean spray velocity was between 2.0 and 2.7 m s$^{-1}$. The instability of the high-speed jets breaks up into small droplets which also undergo evaporation. In one study, droplet sizes were measured for pMDI with CFC and HFA propellants without any active drug. The mean volume droplet size was from 5.2 to 10.8 μm for the HFA formulation and larger droplets were measured for the CFC formulation (60).

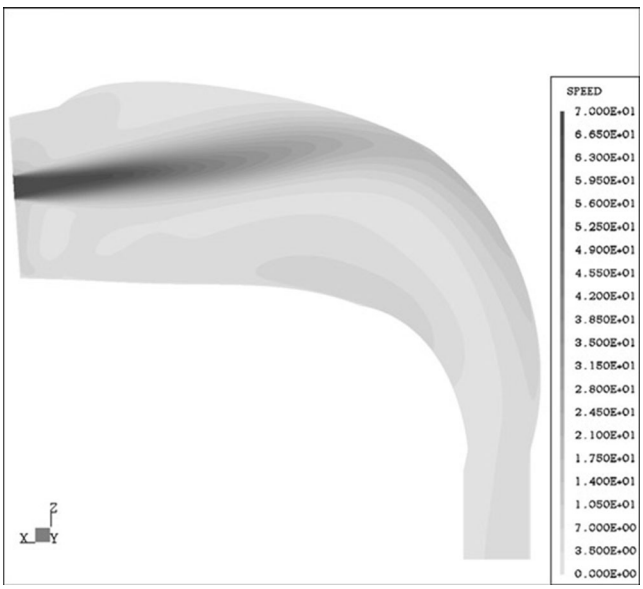


**Fig. 8.** Midplane flow field results for inlet diameter, Din=3.0 mm, and inhalation flow rate, $Q$=32.2 L min$^{-1}$, of dry powder aerosol delivery in an oral airway (with permission from Matida *et al.* (56)

There were two phases in the formation of droplets. In the first phase, the instability of the jet coming from the nozzle forms *primary* droplets. In the second phase, the formation of the smaller *secondary* droplets is due to deformation of the primary droplets (61). Using the couple Euler–Lagrange approach for the gas droplet flow and an Enhanced Taylor Analogy Breakup model assuming the primarily droplet diameter equal to the nozzle diameter, Shi and Kleinstreuer were able to numerically simulate the droplet spray dynamics of several fluids including the droplet size and plume velocity as a function of distance from the nozzle exit (61). This

technique was further combined with the evaporation of the droplet, and a CFD simulation (16) was performed to understand the aerosol deposition of pMDIs onto an oropharyngeal airway with a geometry similar to the one reported by Cheng *et al.* (20). A pMDI with CFC formulation and an actuator valve of 0.5 mm diameter and another with HFA formulation with a valve diameter of 0.25 mm were studied. The inspiratory flow rate was 30 L $min^{-1}$ in both cases. Also, aerosol deposition when the pMDI was connected with a holder chamber was simulated. For the CFC formulation, the dense spray cone distributed droplets fully in the oral cavity with about 90% deposited in the oropharyngeal region. For the HFA formulation, the droplet size was smaller and penetrated the oropharyngeal region much better with 54% deposition in the oropharyngeal airway. This deposition pattern agreed with results obtained *in vivo* (38) and *in vitro* (44).

## NASAL SPRAY

Several types of therapeutic agents, including corticosteroids, vasoconstrictors, and antihistamines, may be delivered to the nasal passages to produce local effects, such as treating rhinitis or allergies (62,63). Various dosage forms have been utilized to deliver medications to the nasal cavity, including drops, powders, nebulized mists, and sprays. Due to their convenience and dose consistency, sprays have become the preferred mode of delivery for nasal products. Nasal delivery is designed to deposit >99% of drug to the nasal cavity. Nasal spray devices producing droplets >40 μm (64,65) would be deposited completely in the nasal cavity following the conventional lung deposition model. An important issue concerning nasal delivery is the distribution of drugs in the nasal cavity, which is divided into three regions including the anterior, turbinate, and posterior regions as shown in Fig. 9. Material deposited in the anterior region including the vestibule and nasal valve can be cleared quickly by sneezing or blowing one's nose. Materials penetrating the nasal valve available for deposition in the turbinate region are desirable. Both gamma scintigraphic measurements in human volunteers and nasal airway replicas have been used to study the deposition pattern of nasal delivery (62–67). These studies identify several key parameters including plume angle, droplet size, plume velocity, and inspiratory flow rate that may influence the deposition pattern of nasal spray devices.

In a gamma scintigraphy study, Newman *et al.* demonstrate that a greater fraction of the total spray volume would penetrate into the ciliate region of the main nasal cavity from a spray whose plume angle was 30° compared to a wider 60° spray (~70 μm median droplet size) (62). *In vitro* tests of the deposition pattern using realistic human nasal replicas provide a simpler and more cost-effective method and yields yet more detailed information. A study of nasal deposition in a realistic nasal replica based on MRI scans of a human volunteer showed the utility of this technique (64). The nasal replica consisted of 77 acrylic plastic sections, 1.5-mm thick, as shown in Fig. 10. Four types of nasal sprays were used with the measure plume angle in parathesis: VP7 (45°), PF 35 (35°), PF 60 (55°), and PF 80 (70°). The volume median droplet diameters were 48.5 for VP7 and between 58 and 62 μm for the PF series spray devices. Figure 11 shows the summary of deposition in the nasal cavity for the four nasal spray devices. Over 99.98% of the material was deposited in the nasal cavity, and the deposition (98%) was concentrated on the anterior and turbinate (middle) regions. VP7 and PF 35 (64.4% and 62.5%) had the highest deposition fraction in the middle region followed by PF 60 (56.5%) and PF 80 (40.4%) indicating that the turbinate deposition efficiency increased with decreasing plume angle.

Using a similar technique and the same nasal replica, Foo *et al.* investigate the effects of droplet size (37 to 158 μm volume median diameter), plume angle (29° to 80°), administration angle above the horizontal (30°, 40°, or 50°), and inspiratory flow (0, 20, and 60 L $min^{-1}$) in three different nasal spray devices (65). Fluids of different viscosity tagged with Rhodamine 590 tetrafluoroborate were used to produce droplets of different sizes and also produce sprays of different plume angles. Their thorough investigation demonstrated that there were minimal effects of droplet size, inspiratory flow, and device type on the deposition pattern. Both plume angle and administration angle were found to be the critical parameters in determining deposition efficiency (Fig. 12). The turbinate deposition decreased with the increasing administration angle. At the smallest angle of 30°, the turbinate deposition is a monotonic decreasing function of plume angle with the maximum deposition reaching 90% for

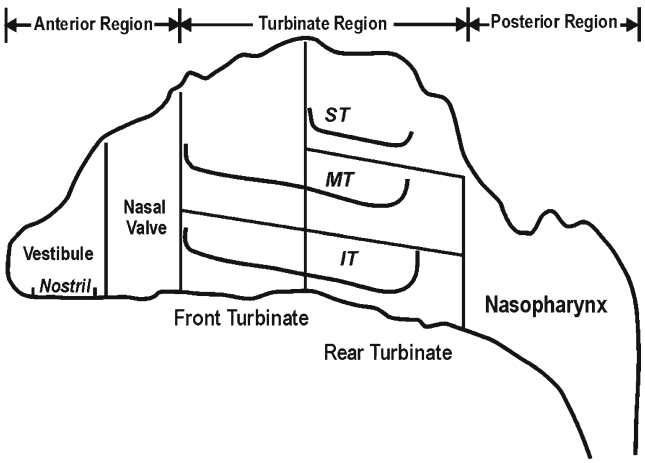


**Fig. 9.** Schematic of a human adult nasal airway

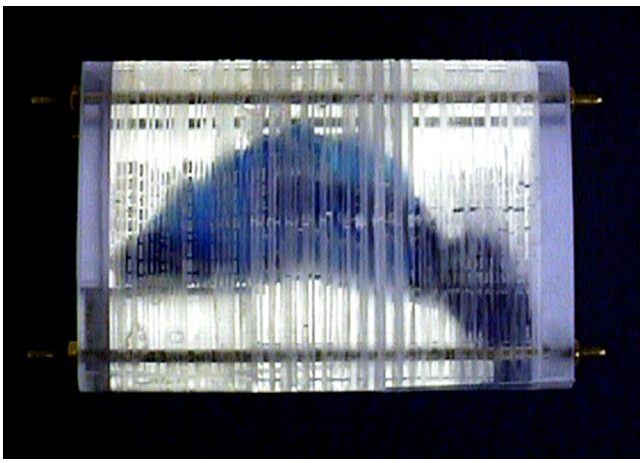

**Fig. 10.** The human multi-sectional nasal airway model

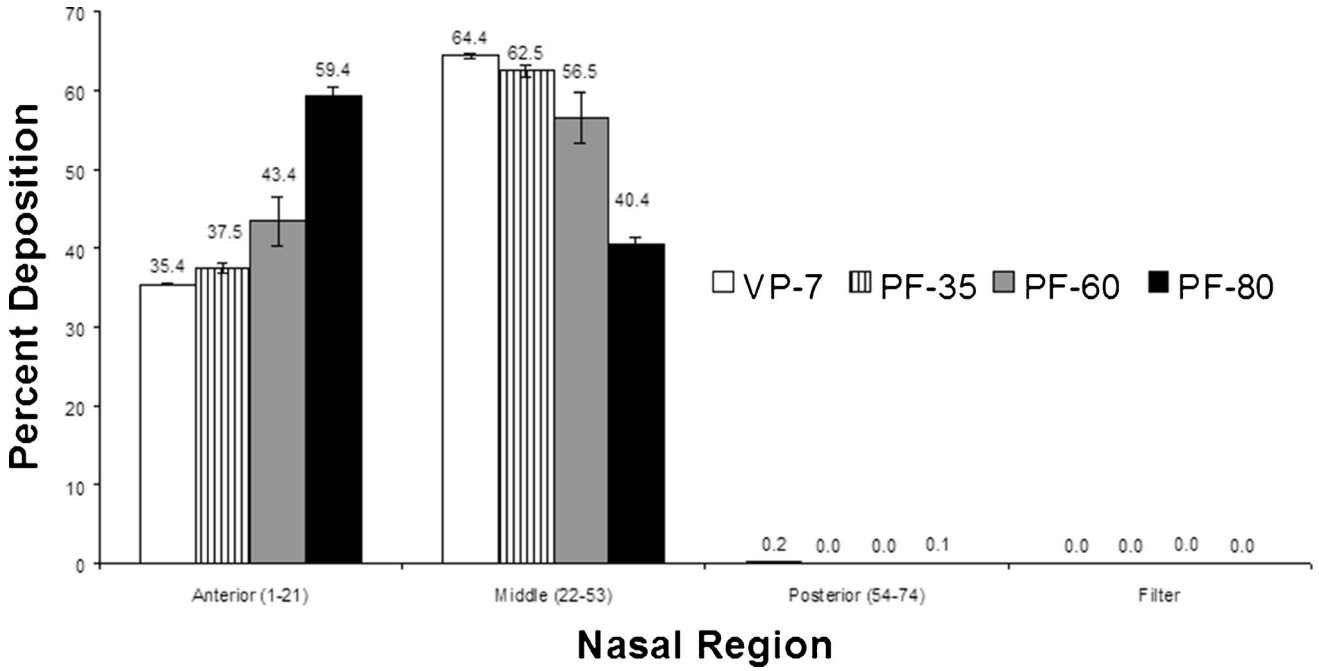


**Fig. 11.** Deposition pattern in the anterior, turbinate, and posterior regions of the nasal airway (with permission from Cheng *et al.* (64))

a small 30° plume angle. For the administration angles of 40° or 50°, the maximum turbinate deposition fraction was 50% and 30%, respectively, at plume angle of 55° to 65°. This study shows that the deposition of large droplets from pump sprays is not affected by the coordinate of spray actuation and nasal breathing because the inspiratory flow has no significant influence on the deposition pattern.

## CONCLUSION

Several types of therapeutic aerosol delivery systems, including pMDI, DPI, nebulizer, the solution mist inhaler, and nasal sprays, are widely used. Both oral and nasal inhalation routes are used for the delivery of therapeutic aerosols. Nasal inhalation is used for nasal sprays to deposit in the nasal cavity, whereas oral inhalation is used for other delivery systems to maximize deposition in the tracheobronchial and alveolar regions. Several methods have been used to estimate the dose to the respiratory tract for pharmaceutical aerosol. FPF obtained from the *in vitro* test of particle size generally correlated with lung deposition fraction obtained from *in vivo* data but did not predict the correct deposition fraction. Aerosol deposition mechanisms in the human respiratory tract have been well studied. Prediction of pharmaceutical aerosol deposition using established lung deposition models has limited success primarily because they underestimated oropharyngeal deposition. Recent studies using realistic upper airway replicas and CFD simulation improved our understanding of aerosol transport and deposition process in the oropharyngeal regions. These studies prove that deposition by the impinging turbulent jet from the narrow diameter of the DPI mouthpiece is the main mechanism for the enhanced deposition in the oropharyngeal region. For pMDI devices, a high-speed jet from the nozzle is responsible for high deposition in the oropharyngeal region. Nasal spray devices producing droplets >40 μm would be deposited completely in the nasal cavity following the conventional lung deposition model. Materials penetrating the nasal valve available for deposition in the turbinate region are desirable. Studies using gamma scintigraphy and nasal airway replicas showed that there were minimal effects of droplet size, inspiratory flow, and device type on the deposition pattern. Both plume angle and administration angle were found to be the critical parameters in determining deposition efficiency.

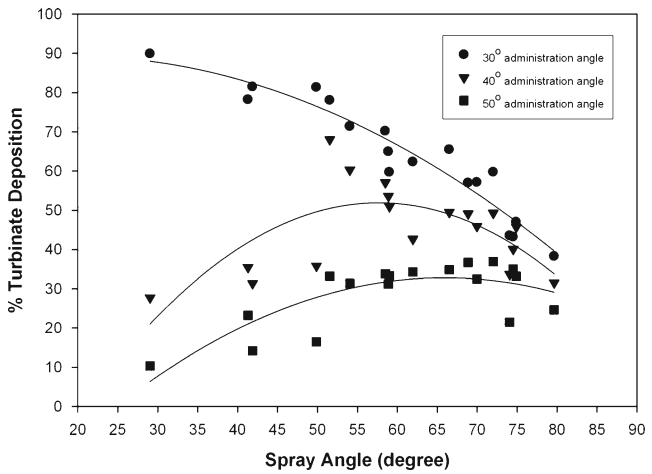


**Fig. 12.** Composite plot of turbinate deposition *versus* plume angle with different administration angles. *Curves* are provided for visualization only. No functional dependence is implied (with permission from Foo *et al.* (65))

## ACKNOWLEDGMENTS

This research was supported by the National Institute for Occupational Safety and Health (NIOSH) contracts 254-2010-M-36304 and 214-2012-M-52048 and NIOSH grants R01 OH009801 and R01 OH010062.

## REFERENCES


1. Newman SP. Can lung deposition data act as a surrogate for the clinical response to inhaled asthma drugs. Br J Clin Pharm. 2000;49:529–37.
2. Derom E, Pauwels R. Relationship between airway deposition and effects for inhaled bronchodilators. In: Dalby R, Byron PR, Farr SJ, editors. Respiratory drug delivery VI. Buffalo Grove: Interpharm Press; 1998. p. 35–44.
3. Cheng YS. Modeling aerosol drug delivery. In: Gradon L, Marijnissen J, editors. Optimization of aerosol drug delivery. Dordrecht: Kluwer; 2003. p. 165–88.
4. Newman S, Bennett WD, Biddiscombe M, Devadason SG, Dolovich M, Fleming J, *et al*. Standardization of techniques for using planar (2D) imaging for aerosol deposition assessment of orally inhaled products. J Aerosol Med Pulmon Drug Deliv. 2012;25:S10–28.
5. Fleming J, Bailey DL, Chan HK, Conway J, Kuehl PJ, Laube BL, *et al*. Standardization of techniques for using single-photon emission computed tomography (SPECT) for aerosol deposition assessment of orally inhaled products. J Aerosol Med Pulmon Drug Deliv. 2012;25:S29–51.
6. ICRP. Human respiratory tract model for radiological protection. London: Pergamon; 1994. Publication 66, Annals of ICRP.
7. NCRP. Deposition, retention, and dosimetry of inhaled radioactive substances. Bethesda: National Council on Radiation Protection and Measurements; 1997. NCRP Report No. 125.
8. Anjilvel S, Asgharian B. A multiple-path model of particle deposition in the rat lung. Fund Appl Toxicol. 1995;28:41–50.
9. Ali M. Pulmonary drug delivery. In: Kulkarni V, editor. Handbook of non-invasive drug delivery systems. New York: Elsevier; 2010. p. 209–46.
10. Martonen TB. Mathematical model for the selective deposition of inhaled pharmaceuticals. J Pharm Sci. 1993;82:1191–9.
11. Pritchard JN, Layzell GR, Miller JF. Correlation of cascade impactor data with measurements of lung deposition for pharmaceutical aerosols. In: Drug delivery to the lungs VII. London: The Aerosol Society; 1996. p. 101–4.
12. Price A. Validation of aerosol deposition models for pharmaceutical purposes: the way forward. In: Dalby R, Byron PR, Farr SJ, Peart J, editors. Respiratory drug delivery VII. Buffalo Grove: Interpharm Press; 2000. p. 197–208.
13. Clark AR, Newman SP, Dasovich N. Mouth and oropharyngeal deposition of pharmaceutical aerosols. J Aerosol Med. 1998;11:S116–21.
14. DeHaan WH, Finlay WH. In vitro monodisperse aerosol deposition in a mouth and throat with six different inhalation devices. J Aerosol Med. 2001;14:361–7.
15. DeHaan WH, Finlay WH. Predicting extrathoracic deposition from dry powder inhalers. J Aerosol Sci. 2004;35:309–31.
16. Kleinstreuer C, Shi HW, Zhang Z. Computational analyses of a pressurized metered dose inhaler and a new drug-aerosol targeting methodology. J Aerosol Med. 2007;20:294–304.
17. Stahlhofen W, Gebhart J, Heyder J. Experimental determination of the regional deposition of aerosol particles in the human respiratory tract. Am Ind Hyg Assoc J. 1980;41:385–98.
18. Emmett PC, Aitken RJ, Hannan WJ. Measurements of the total and regional deposition of inhaled particles in the human respiratory tract. J Aerosol Sci. 1982;13:549–60.
19. Heyder J, Gebhart J, Rudolf G, Schiller CF, Stahlhofen W. Deposition of particles in the human respiratory tract in the size range of 0.005-15 um. J Aerosol Sci. 1986;17:811–25.
20. Cheng YS, Zhou Y, Chen BT. Particle deposition in a cast of human oral airways. Aerosol Sci Technol. 1999;31:286–300.
21. Smith SM, Cheng YS, Yeh HC. Deposition of ultrafine particles in human tracheobronchial airways of adults and children. Aerosol Sci Technol. 2001;35:697–709.
22. Zhou Y, Cheng YS. Particle deposition in a cast of human tracheobronchial airways. Aerosol Sci Technol. 2005;39:492–500.
23. Asgharian B, Price OT. Deposition of ultrafine (nano) particles in the human lung. Inhal Toxicol. 2007;19:1045–54.
24. Phalen RF, Hinds WC, John W, Lioy PJ, Lippmann M, McCawley MA, *et al*. Rationale and recommendations for particle size-selective sampling in the workplace. Appl Ind Hyg. 1986;1:3–12.
25. Soderholm SC. Proposed international conventions for particle size-selective sampling. Ann Occup Hyg. 1989;33:301–20.
26. Kwok PCL, Chan HK. Electrostatics of pharmaceutical inhalation aerosols. J Pharma Pharmacol. 2009;61:1587–99.
27. Melandri C, Tarroni G, Prodi V, DeZaiacomo T, Formignani M, Lomardi CC. Deposition of charged particles in the human airway. J Aerosol Sci. 1983;14:657–69.
28. Yu CP. Precipitation of unipolarly charged particles in cylindrical and spherical vessels. J Aerosol Sci. 1977;8:237–42.
29. Yu CP, Chandra K. Depoition of charged particles from laminar flows in rectangular and cylindrical channels by image force. J Aerosol Sci. 1978;9:175–80.
30. Cohen BS, Qiong JQ, Fang CP, Li W. Deposition of charged particles on lung airways. Health Phys. 1998;74:554–60.
31. Hickey AJ, Martonen TB, Yang Y. Theoretical relationship of lung deposition to the fine particle fraction of inhalation aerosols. Pharmceutica Acta Helvetiae. 1996;71:185–90.
32. Newman SP. How well do in vitro particle size measurements predict drug delivery in vivo. J Aerosol Med. 1998;11:S97–S104.
33. Marple VA, Olson BA, Miller NC. The role of inertial particle collectors in evaluating pharmaceutical aerosol delivery systems. J Aerosol Med. 1998;11:S139–53.
34. Agnew JE. Characterizing lung aerosol penetration. J Aerosol Med. 1991;4:237–49.
35. Clark AR. In vitro assessment of spacers and reservoir devices. In: Dalby R, Evans R, editors. Respiratory drug delivery II. Boca Raton: CRC Press; 1990. p. 27–31.
36. Newman SP, Pitcairn G, Hooper G, Knoch M. Efficient drug delivery to the lungs from a continuously operated open-vent nebulizer and low pressure compressor system. Eur Respir J. 1994;7:1177–81.
37. Barry PW, O'Callaghan C. In vitro analysis of the output of salbutamol from different nebulizers. Eur Respir J. 1999;1130:1164–9.
38. Leach CL, Davidson PJ, Bouhuys A. Improved airway targeting with the CFC-free HFA-beclomethasone metered-dose inhaler compared with CFC-beclomethasone. Eur Respir J. 1998;12:1346–53.
39. Newman SP, Moren F, Trofast E, Talaee N, Clarke SW. Deposition and clinical efficiency of terbutaline sulphate from turbuhaler, a new multi-dose powder inhaler. Eur Respir J. 1989;2:247–52.
40. Newman SP, Clarke AR, Talaee N, Clarke SW. Pressurized aerosol deposition in the human lung with and without an "open" spacer device. Thorax. 1989;44:706–10.
41. Newman SP, Clarke AR, Talaee N, Clarke SW. Lung deposition of 5 mg Intal from a pressurized metered dose inhaler assessed by radiotracer technique. Int J Pharm. 1991;74:203–8.
42. Richards J, Hirst P, Pitcairn G, Mahashbde S, Abramowitz W, Nolting A, *et al*. Deposition and pharmacokinetics of flunisolide delivered from pressurized inhalers containing non-CFC and CFC propellants. J Aerosol Med. 2001;14:197–208.
43. Hirst PH, Pitcairn G, Weers JG, Tarara TE, Clark AR, Dellamary LA, *et al*. In vivo lung deposition of hollow porous particles from a pressurized metered dose inhaler. Pharmaceut Res. 2002;19:258–63.
44. Cheng YS, Fu C, Yazzie D, Zhou Y. Respiratory deposition patterns of salbutamol pMDI with CFC and HFA-134a formulations in a human airway replica. J Aerosol Med. 2001;14:255–66.
45. Zhang Y, Gilbertson K, Finlay WH. In vivo-in vitro comparison of deposition in three mouth-throat models with Qvar® and Turbuhaler® inhalers. J Aerosol Med. 2007;20:227–35.
46. Borgstrom L, Bondesson E, Moren F, Trofast E, Newman SP. Lung deposition of budesonide inhaled via Turbuhaler: a comparison with terbutaline sulphate in normal subjects. Eur Respir J. 1994;7:73.
47. Newman SP, Pitcairn G, Adkin DA, Vidgren MT, Silvasti M. Comparison of beclomethasone dipropionate delivery by Easyhaler dry powder inhaler and PMDI plus large volume spacer. J Aerosol Med. 2001;14:217–25.
48. Pitcairn GR, Lunghetti G, Ventura P, Newman S. A comparison of the lung deposition of salbutamol inhaled from a new dry powder inhaler at two inhaled flow rates. Int J Pharma. 1994;102:11–8.
49. Pitcairn GR, Lankinen T, Valkila E, Newman SP. Lung deposition of salbutamol inhaled from the Leiras metered dose powder inhaler. J Aerosol Med. 1995;8:307–11.

50. Cheng KH, Cheng YS, Yeh HC, Swift DL. Measurements of airway dimensions and calculation of mass transfer characteristics of the human oral passage. J Biomed Eng. 1997;119:475–82.
51. Kleinstreuer C, Zhang ZQ. Laminar-to-turbulent fluid-particle flows in a human airway model. Int J Multi Flow. 2003;29:271–89.
52. Zhang Z, Kleinstreuer C, Kim CS, Cheng YS. Vaporizing microdroplet inhalation, transport, and deposition in a human upper airway model. Aerosol Sci Technol. 2004;38:36–49.
53. Fadl A, Wang J, Zhang Z, Cheng YS. Effects of MDI spray angle on aerosol penetration efficiency through an oral airway cast. J Aerosol Sci. 2007;38:865–84.
54. Xi J, Longest PW. Transport and deposition of micro-aerosols in realistic and simplified models of the oral airway. Ann Bio Eng. 2007;35:560–81.
55. Stapleton KW, Guentsch E, Hoskinson MK, Finlay WH. On the suitability of k-ε turbulence modeling for aerosol deposition in the mouth and throat: a comparison with experiment. J Aerosol Sci. 2000;31:739–49.
56. Matida EA, DeHaan WH, Finlay WH, Lange CF. Simulation of particle deposition in an idealized mouth with different small diameter inlets. Aerosol Sci Technol. 2003;37:924–32.
57. Gric B, Finlay WH, Burnell PKP, Heenan AF. In vitro intersubject and intrasubject deposition measurements in realistic mouth-throat geometries. J Aerosol Med. 2004;35:1025–40.
58. Zhou Y, Sun JJ, Cheng YS. Comparison of deposition in the USP and physical mouth-throat models with solid and liquid particles. J Aerosol Med Pulmon Drug Deliv. 2011;24:277–84.
59. Hochrainer D, Holz H, Kreher C, Scaffidi L, Spallek M, Wachtel H. Comparison of the aerosol velocity and spray duration of Respimat soft mist inhaler and pressurized metered dose inhalers. J Aerosol Sci. 2005;18:273–82.
60. Dunbar CA, Watkins AP, Miller JF. An experimental investigation of the spray issued from a pMDI using laser diagnostic techniques. J Aerosol Med. 1997;10:351–68.
61. Shi HW, Kleinstreuer C. Simulation and analysis of high-speed droplet spray dynamics. J Fluid Eng. 2007;129:621–33.
62. Newman SP, Moren F, Clarke SW. Deposition pattern of nasal sprays in man. Rhinol. 1987;26:111–20.
63. Thorsson L, Newman SP, Weisz A, Trofast E, Moren F. Nasal distribution of budesonide inhaled via a powder inhaler. Rhinol. 1993;31:7–10.
64. Cheng YS, Holmes TD, Gao J, Guilmette RA, Li S, Surakitbanharn Y, *et al*. Characterization of nasal spray pumps and deposition pattern in a replica of the human nasal airway. J Aerosol Med. 2001;14:267–70.
65. Foo MY, Cheng YS, Su WC, Donovan MD. The influence of spray properties on intranasal deposition. J Aerosol Med. 2007;20:495–508.
66. Suman JD, Laube BL, Lin C, Brouet G, Dalby R. Validity of in vitro tests on aqueous spray pumps as surrogates for nasal deposition. Pharmaceut Res. 2002;19:1–6.
67. Al-Ghananeem AM, Sandefer EP, Doll WJ, Page RC, Chang Y, Digenis GA. Gamma scintigraphy for testing bioequivalence: a case study on two cromolyn sodium nasal spray preparations. Int Pharm. 2008;357:70–6.